

UKAEA-CCFE-PR(22)55

JW Berkery, SA Sabbagh, L Kogan, S Gibson, D  
Ryan, V Zamkovska, J Butt, J Harrison, S  
Henderson, MAST-U team

# **Operational Space of the First Physics Campaign of MAST-U**

Enquiries about copyright and reproduction should in the first instance be addressed to the UKAEA Publications Officer, Culham Science Centre, Building K1/O/83 Abingdon, Oxfordshire, OX14 3DB, UK. The United Kingdom Atomic Energy Authority is the copyright holder.

The contents of this document and all other UKAEA Preprints, Reports and Conference Papers are available to view online free at [scientific-publications.ukaea.uk/](https://scientific-publications.ukaea.uk/)

# Operational Space of the First Physics Campaign of MAST-U

JW Berkery, SA Sabbagh, L Kogan, S Gibson, D Ryan, V Zamkovska, J Butt, J Harrison, S Henderson, MAST-U team



# Operational Space of the First Physics Campaign of MAST-U

J W Berkery<sup>1</sup>, S A Sabbagh<sup>2</sup>, L Kogan<sup>3</sup>, S Gibson<sup>3</sup>, D Ryan<sup>3</sup>, V Zamkovska<sup>2</sup>, J Butt<sup>2</sup>, J Harrison<sup>3</sup>, S Henderson<sup>3</sup>, and the MAST-U team\*

<sup>1</sup> Princeton Plasma Physics Laboratory, Princeton, NJ 08543, United States of America

<sup>2</sup> Department of Applied Physics and Applied Mathematics, Columbia University, New York, New York 10027, USA

<sup>3</sup> Culham Centre for Fusion Energy, UKAEA, Abingdon, OX14 3DB, UK

\* See author list of Harrison J R *et al* 2019 *Nucl. Fusion* **59** 112011

E-mail: [jberkery@pppl.gov](mailto:jberkery@pppl.gov)

Received xxxxxx

Accepted for publication xxxxxx

Published xxxxxx

## Abstract

The MAST-U fusion plasma research device, the upgrade to the Mega Amp Spherical Tokamak, has recently completed its first campaign of physics operation. MAST-U operated with Ohmic, or one or two neutral beams for heating, at 400-800 kA plasma current, in conventional or “SuperX” divertor configurations. Equilibrium reconstructions provide key plasma physics parameters vs. time for each discharge, and diagrams are produced which show where the prevalence of operation occurred as well as the limits in various operational spaces. When compared to stability limits, the operation of MAST-U so far has generally stayed out of the low  $q$ , low density instability region, and below the high density Greenwald limit, high beta global stability limits, and high elongation vertical stability limit. MAST-U still has the potential to reach higher elongation, which could benefit the plasma performance.

Keywords: spherical tokamak, operational space

(Some figures may appear in colour only in the online journal)

## 1. Introduction

The upgrade to the fusion research device Mega Amp Spherical Tokamak (MAST) [1], called MAST-U [2], was years in the making, but recently completed its first physics campaign [3]. One of the main goals of research in MAST-U is to exploit the new capabilities of the upgrade, including new poloidal magnetic field coils and a flexible divertor geometry, to study the performance of fusion plasmas in unique configurations. To this end, it is important to track the operational space of the plasmas in the device in the multidimensional space of various key physics parameters.

The equilibrium states of magnetically confined plasmas are stable balance points between magnetic and plasma pressures. These equilibria must be reconstructed from diagnostic measurements of the plasma conditions [4]. Once the

equilibrium reconstruction is performed, many important plasma parameters, such as the shape of the enclosing flux surfaces and the pressure, are known. Measurements of density and temperature of the electron and ion components add to the knowledge of its state at a given time during a discharge. Typically in fusion devices the plasma current is ramped up, held at a steady level during the “flattop”, and then ramped down again if it has not been disrupted by various modes of instability of the plasma. In the first campaign of MAST-U the flattop current was between roughly 400-800 kA and lasted on the order of a half to one second.

One of the goals of fusion research devices is to explore the parameter space and the limits of magnetically confined plasma operation to see where plasmas can be stably operated without disruption. These limits can be compared to theoretical expectation and used to project to future devices.

$I_p$ (kA)	Divertor	Ohmic	SW	SS	2B
400	CD	148		12	
	SX	64			
	UN	44			
600	CD	39	9	25	7
	SX	56	12		8
	UN	16		6	
700	CD	53	77	31	108
	SX	68			
	UN	30	31	3	9

**Table 1.** Number of discharges in the MAST-U first campaign database, split by plasma current, divertor geometry, and heating level. Note this does not represent every discharge of the campaign. “400” contains ~400-450 kA plasmas and “700” ~700-750 kA.

A straightforward way to do this is to create operational space diagrams, which show the frequency of operation at a given value of key plasma parameter over the course of a months or years long campaign of experimentation. The Disruption Event Characterization and Forecasting (DECAF) code [5,6], which analyses the chains of events that lead to disruptions and their patterns in multiple machine databases, is also equipped to provide operational space diagrams.

The underlying data that DECAF uses to produce these diagrams, for MAST-U, come from the EFIT++ equilibrium reconstruction code [7,8], which presently uses magnetics data only as an input. Kinetic profiles from Thomson scattering were routinely available, and charge exchange recombination spectroscopy and motional Stark effect diagnostics were also available for most discharges with the “south” neutral beam injection, but using these in equilibrium reconstructions is a work in progress [8]. Additionally, the requested plasma current from the plasma control system [9], the measured plasma current, and the measured line density are used.

The measurements, reconstructed variables, and DECAF analysis results were stored in SQL databases on computers at the Princeton Plasma Physics Laboratory (PPPL) for easy access for the U.S. based researchers.

## 2. The MAST-U database

MAST-U was operated in various set discrete allowed scenarios in three main categories, which are logged for each discharge: the plasma current level, the shape of the divertor, and the level of neutral beam heating. Besides a small number of limiter discharges where the closed flux surfaces impact on a metal “limiting” structure in the machine, which we will exclude, all MAST-U discharges ran in the double null (DN)

configuration, where magnetic field coils are used to pull the open field lines beyond the last closed flux surface to divertor targets at both the top and bottom of the machine. Therefore we can categorize all MAST-U discharges into 24 categories based on the choice of three plasma current request levels, two divertor geometries, and four levels of beam heating. The three current levels used were 400-450, 600, and 700-750 kA. The two divertor geometries were conventional (CD) and super-X (SX) [10], however in a number of cases the divertor configuration was unspecified (UN). There were also just a couple of “snowflake” divertor discharges in the first campaign as well, but these were not included. Finally the four heating levels were Ohmic (OH, no beams), one beam from the “southwest” beam (SW), one beam from the “south” beam (SS), and two beams (2B). Therefore, every discharge in MAST-U is, in principle, labelled by the session leader after it is performed in a scenario, such as: DN-700-SX-1BSW. This categorization is done on a shot level, and while it can be assumed that the current is maintained at a steady level, there is no guarantee that the SX divertor was maintained during that time, nor that the SW beam was on for the full flat-top duration (often it was not). Additionally, the achieved plasma current could differ from the request, especially early in the run before Rogowski coil calibrations were updated (in one extreme example 810kA was achieved for a programmed 750kA discharge).

Nevertheless, these are convenient categories to split the discharges to look at differences in their operational spaces. Some discharges were not labelled at the time of their operation, in which case we have retroactively categorized them by current and beam heating, but not by divertor geometry. Automatic evaluation of the strike point location to determine the time and position of the SX divertor flux expansion is being developed. Comparisons between the strike point location from equilibrium reconstruction and peak heat flux locations or Langmuir probe data are also being made [8].

Finally, the scenario listed in the session logs reflects the programmed scenario, but it doesn’t always reflect what was achieved. For example, if a discharge was labelled as 2B, but only one beam fired while the other malfunctioned, we have recategorized it into the appropriate scenario. In fact, many of discharges with the SW beam only were meant to be 2B discharges, but the SS beam did not fire properly.

The database of MAST-U discharges derived from the magnetics-only equilibrium reconstructions utilized here for the operational space diagrams does not include every plasma discharge. Discharges before June, 2021 were excluded as the machine was in an early phase of operation. In the discharges used, in the range of shot numbers 44114-45484 from the months of June-October, 2021, there were some “fizzle” cases that did not make it to the current flat-top, some cases where

not all the necessary data was available to run the reconstruction, and finally cases in which the equilibrium reconstruction was run but the  $\chi^2$  number indicating the goodness of the fit of the reconstruction to all the data that goes into it was too high ( $> 30$ ). We are left with a total of 855 discharges, separated into the different scenarios according to Table 1. In each discharge, the flattop was split into 5 ms intervals, so that for every second of flattop in a discharge, 200 individual equilibrium times are taken. This way the total number of equilibria in the database was 108,826. A majority of the discharges, and equilibria, in the first campaign had Ohmic heating only, and the two most frequent conventional divertor scenarios were at the extremes: low current Ohmic, and high current two beam.

Finally, there are obvious gaps in the scenario map in table 1. For example, there are no discharges with the SW beam in 400kA plasmas. This is by choice, as the confinement of the SW beam energetic particles, which are injected off-axis, was deemed to be too poor in lower current discharges, so they were not attempted.

### 3. Operational space diagrams

In general, the DECAF code can produce diagrams showing the probability of any DECAF event, such as disruption, Greenwald limit, vertical displacement event, etc... occurring within a given parameter space of tokamak operation [6]. Diagrams showing the frequency of disruption [11] and magnetic island widths [12] have been previously produced for the database of MAST discharges. Here however, we present DECAF-produced operational space diagrams, which more simply show the number of times the plasmas accessed a given space. A limited number of such diagrams have been independently illustrated for MAST-U in Ref. [3].

Operational space plots are useful for showing where the plasmas generally operate and the boundaries of that operation. Each square of parameter space is plotted with a color on a logarithmic scale ranging from 1 (blue) to 1000 (yellow) indicating how many equilibrium points from the database exist within that space. This way the density of operation in a given space is illustrated. Usually such diagrams are made with scatter plots of points, which does not show this, or sometimes with shading, which does but only qualitatively (some examples from MAST are in Refs. [13,14,15]). Generally, in the following, the two dimensional spaces illustrated have a resolution of a 50 x 50 square grid. Squares are only plotted if they have 3 or more equilibria in them.

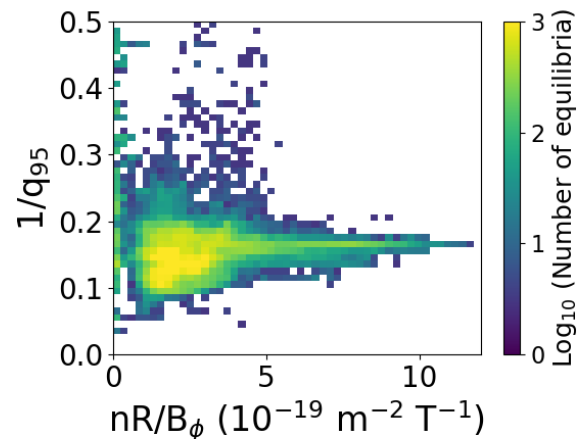


**Figure 1:** Hugill diagram of the operational space of the first campaign of MAST-U.

#### 3.1 Hugill diagram

A well-known diagram in fusion plasma physics is the Hugill diagram [16], which plots tokamak operation in the space of  $nR/B_\phi$  vs.  $1/q_{95}$ . Here,  $n$  is the line average density,  $R$  is the major radius of the magnetic axis,  $B_\phi$  is the toroidal magnetic field at axis, and  $q_{95}$  is the safety factor at 95% of the magnetic flux. The advantage of this diagram is that it shows both a low  $q$  limit due to current driven instabilities as a horizontal line on the plot, for example as  $q_{95} = 2$  (at  $1/q_{95} = 0.5$ ), and a density limit as a diagonal line on the plot. The density limit is perhaps more intuitively shown in a different Greenwald diagram which will be discussed next. Figure 1 shows the Hugill diagram for MAST-U. As a spherical tokamak, MAST-U generally has quite high edge safety factor, as can be seen in the figure where almost all of the operation is between  $5 < q_{95} < 10$ . It should be noted that in limited equilibrium reconstructions including a measurement of magnetic pitch angle from the motional Stark effect diagnostic, the  $q$  profile can be generally shifted slightly ( $\sim 0.5$ ) lower than for magnetics only reconstructions [8], but this isn't anticipated to make a large difference in the conclusions of the Hugill diagram.

So far MAST-U has operated below any low  $q$  stability limits. In MAST disruptivity was elevated generally in the upper left region, above  $1/q_{95} \sim 2$  and below  $nR/B_\phi \sim 5$  [11]. Some discharges in MAST-U have suffered from low density locked modes, however. This sometimes occurred because the density was often kept low on purpose for example in Ohmic plasmas in order to get power into the divertor for dedicated divertor experiments.

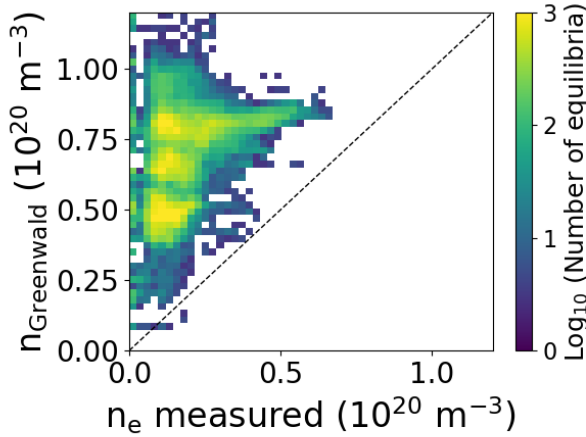


**Figure 2:** Greenwald diagram of the operational space of the first campaign of MAST-U. The dashed line shows the Greenwald limit.

### 3.2 Greenwald limit diagram

Tokamak fusion plasmas have long been known to be subject to a density limit where the line average density  $n_e$  [ $10^{20}\text{m}^{-3}$ ] is limited to the so-called Greenwald density  $n_G \equiv I_p/\pi a^2$ , where  $I_p$  is the plasma current in MA and  $a$  is the plasma minor radius in m [17]. An easy way to illustrate this limit is to simply plot the measured density against the Greenwald density, and a diagonal line indicates the limit. In some ways this diagram is a reconfiguration of the Hugill diagram [18], because the vertical axis is proportional to plasma current, so theoretically this diagram shows a current limit at the top. Additionally, at low density on the left there is a possibility to see a low density runaway electron boundary, but this area is small on the diagram.

Figure 2 shows that MAST-U has generally stayed well under the Greenwald limit in the flattop to this point. Lower plasma current discharges need to maintain a lower density to stay under the limit, as illustrated in Fig. 3 where the database is split into the three plasma current levels with colored line contours containing a minimum of 30 equilibria. This doesn't show the detail of where operation was more prevalent in that space, but rather a general envelope of the operation. This style of plot uses a lower resolution plotting grid of  $25 \times 25$  squares for less detail in the contours, to make the plot more readable.

As was mentioned, the plasma density was often relatively low in the first MAST-U campaign. Additionally, it was seen that the optimal Greenwald fraction for maximizing the plasma stored energy was about 0.6 [3]. However, there were occasional cases of flattop plasmas crossing the Greenwald limit, leading to disruption, for example 400kA Ohmic discharges which reached a Greenwald limit at  $0.4 \times 10^{20}\text{m}^{-3}$ , as indicated in Fig. 2 where the operational space touches the line. These can not be seen in Fig. 3 because there are less than

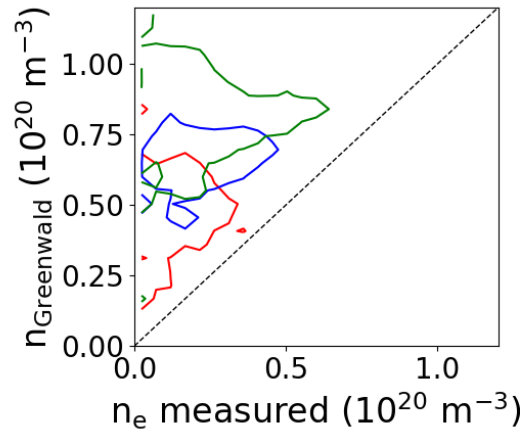


**Figure 3:** Greenwald diagram of the operational space of the first campaign of MAST-U. The lines are contours containing at least 30 equilibria for: 400kA (red), 600kA (blue), and 700kA (green).

30 such cases. There were also purposeful ramps in density in some discharges in the first campaign. These individual probes of the density limit will be the subject of a future more focused study, comparing experiment to theories, such as a newly proposed limit formulation based on boundary turbulent transport [19].

Finally, the  $I_p$  rampdown phase was not included in the database shown here, but it can lead to cases of plasmas crossing the Greenwald limit because the limit comes down with  $I_p$ . One way to combat this is to purposefully shrink the plasma, so that the reducing  $a$  counteracts the reducing  $I_p$ . This strategy has been employed successfully in some discharges in MAST-U.

### 3.3 Normalized beta diagrams

Another traditional diagram in fusion plasma physics that in principle shows more than one operational limit is a plot showing  $\langle\beta_i\rangle$  vs.  $l_i I_p/(aB_0)$ . Here  $l_i$  is the plasma internal inductance,  $l_i \equiv \langle B_p^2 \rangle / B_p^2(a)$  (where  $B_p$  is the poloidal magnetic field), which indicates peaking of the current profile. The plasma current here is in units of MA and  $a$  is the minor radius in m.  $\beta_i$  is the toroidal beta, a ratio of plasma pressure to magnetic pressure defined by  $\beta_i \equiv 2\mu_0 \langle p \rangle / B_0^2$ , where  $\langle p \rangle$  is the volume-average plasma pressure. Clearly, from Fig. 4, much of the MAST-U operation so far has been at lower beta, which is consistent with what was seen in Table 1, that the majority of plasmas so far have Ohmic heating only.

The macroscopic stability of fusion plasmas is known to decrease with an increasing ratio of normalized beta to internal inductance, although not necessarily monotonically [20]. Conveniently, since  $\beta_N \equiv \langle\beta_i\rangle a B_0 / I_p$ , diagonal lines on this diagram represent levels of  $\beta_N / l_i$ . Figure 4 shows that the operational space of MAST-U reaches  $\beta_N / l_i = 3.3$  so far. This is well below the so-called no-wall limit, which was projected

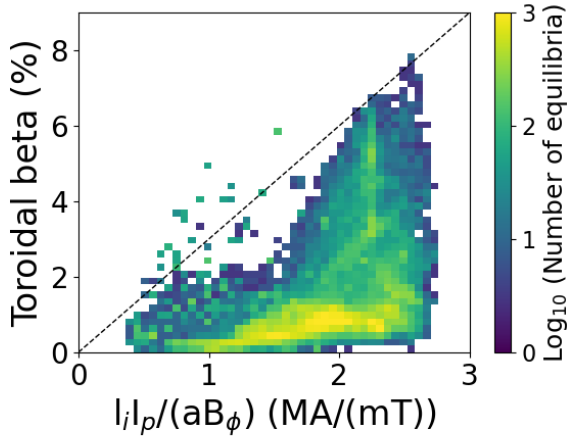


**Figure 4:**  $\langle \beta_t \rangle$  vs.  $l_i I_p / (a B_0)$  diagram of the operational space of the first campaign of MAST-U. The dashed line shows  $\beta_N / l_i = 3$ .

to be about  $\beta_N / l_i = 7$  for MAST-U [21]. Above this limit resistive wall modes can become unstable without stabilizing effects, although modelling for MAST suggests that kinetic stabilization may be sufficient to maintain stability [22].

Secondly this same diagram is meant to show a low  $q$  operational limit as the abscissa approaches 4. Once again, the MAST-U operation is well below this limit as of yet.

A more straightforward way of showing the macroscopic stability limit is a  $\beta_N$  vs.  $l_i$  diagram. This is simply another way of displaying the same information. Such diagrams from the early operating days of MAST showed plasmas reaching  $\beta_N / l_i$  of 6 [13,15]. Figure 5 shows the data plotted this way, again indicating the maximum  $\beta_N / l_i$  so far in early operation of MAST-U is about 3.3. The maximum transient values in the database of  $\beta_N / l_i = 3.37$  and  $\beta_N = 3.47$  (both from discharge 45477) cannot be seen in this diagram because equilibria with  $\beta_N > 2.8$  were too rare.

Not surprisingly, the highest  $\beta_N$  operating points came during plasmas with both neutral beams injected. This can be seen in Fig. 5, where a steady increase in  $\beta_N$ , and general decrease in  $l_i$ , is seen from Ohmic to beam operation. A similar pattern was noted early in MAST operation [13]. Naturally, plasma stored energy increased with increased injected power in MAST-U [3]. Additionally, performance increased from SW to SS to 2B operation. The reason that the SS beam can generally lead to higher  $\beta_N$  plasmas than the SW beam is that it is oriented to deposit energy on-axis, while the SW beam is off-axis.

One of the major focuses of the MAST-U program is to develop the super-X divertor for heat and power exhaust handling in a spherical tokamak. One can see from Table 1 that the SX has been mostly operated in OH plasmas to date, with just a few one and two beam discharges. A key

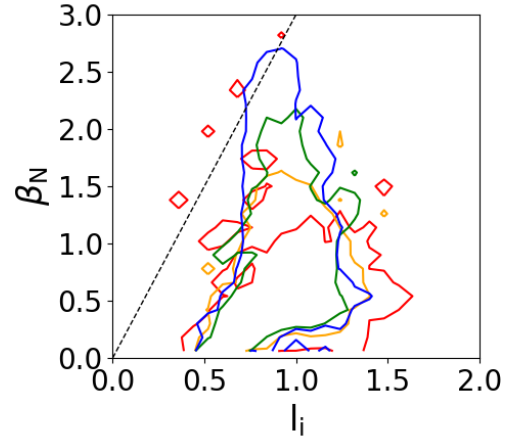


**Figure 5:**  $\beta_N$  vs.  $l_i$  diagram of the operational space of the first campaign of MAST-U. The dashed line shows a  $\beta_N / l_i$  level of 3. The colored lines are contours containing at least 30 equilibria for: OH (red), SW (orange), SS (green), and 2B (blue).

consideration is whether the divertor configuration affects the core plasma. Though it's not shown in the diagrams presented here, by comparing the achieved range of normalized beta between CD and SX Ohmic plasmas, at each of the plasma current levels, we have seen that there is no discernable difference so far between the CD and SX plasmas with respect to the core plasma pressure. Though there have been short periods of H-mode confinement obtained in SX plasmas, sustained and systematic SX H-modes were not a focus of the first campaign, so a comparison between CD and SX core plasmas in H-mode will be a future consideration.

### 3.4 Vertical stability

Elongated plasmas are potentially prone to vertical instability, in which control of the plasma position is lost and it either moves upwards or downwards until striking the surrounding material. Lower aspect ratio plasmas naturally have a higher elongation,  $\kappa$ , but there is a limit on that elongation that can be stably maintained, which is inversely proportional to the internal inductance [23]. Improvements to vertical stability control, of course, increase the achievable  $\kappa$  for a given  $l_i$  [24]. By the time a disruption of the plasma current has occurred due to the vertical instability process, the plasma may have shrunk to a lower  $\kappa$  and increased its  $l_i$ , but the originating vertical displacement event generally begins at higher  $\kappa$ , lower  $l_i$ . [6,23].

Figure 6 shows that MAST-U plasmas operated as expected – lower  $l_i$  plasmas had higher  $\kappa$  [3]. The dashed line shown is an upper limit of  $\kappa = 3.4 - l_i$  derived from the experience of NSTX for design of future spherical tokamaks [25]. A boundary such as this has been proposed for a model predictive control scheme for tokamaks [26]. This indicates that MAST-U still potentially has some margin to increase the

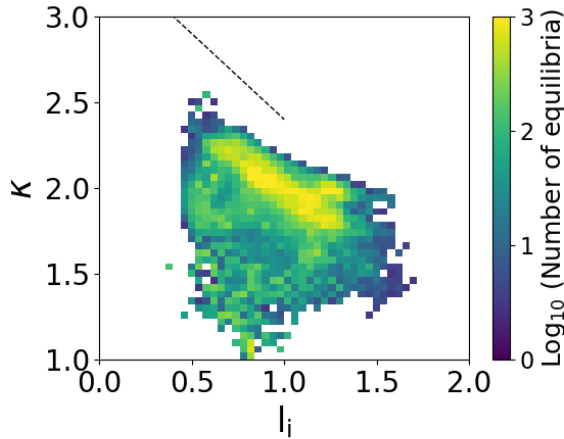


**Figure 6:**  $\kappa$  vs.  $l_i$  diagram of the operational space of the first campaign of MAST-U. The dashed line shows  $\kappa = 3.4 - l_i$ .

elongation of its plasmas, especially as  $l_i$  is lowered even further in future campaigns. It should be noted, however, that the operational space achieved in the NSTX database of discharges was somewhat lower than the limit derived and shown.

### 3.5 Plasma performance improvement from plasma shaping

With the exception of vertical stability, increased elongation in spherical tokamaks tends to increase the stability of the plasmas. Additionally, it is associated with improved confinement of the plasma energy. In fact, fusion power output scales approximately with elongation, normalized beta, and toroidal field all to the fourth power, so increases in elongation are quite important for spherical tokamaks [25].

Another way of considering the importance of elongation is to consider that increased elongation allows for the increase in the product of toroidal beta and bootstrap current (non-inductive current) fraction. These two parameters are both important –  $\beta_t$  for fusion gain and  $f_{bs}$  for pulse length and sustainment of the discharge, but they are inherently competitive through the relation  $f_{bs}\beta_t \sim A^{-1/2}(1+\kappa^2)\beta_N^2$  [25,27]. An increase of  $\kappa$  increasing the product of these parameters, however, means the ability to either simultaneously increase both or to increase one without detriment to another. The fraction of current being carried by the bootstrap effect can be determined per shot by analysis, but since bootstrap fraction scales with poloidal beta, it was recognized that a convenient way to visualize this benefit of elongation with global parameters was to plot  $\beta_p\beta_t$  vs.  $1+\kappa^2$  [24].

Figure 7 shows this diagram for the first campaign of MAST-U. The units of the ordinate are not important (in our case the  $\beta_t$  was in percentage while the  $\beta_p$  was not). What is important is the increase in value as elongation increases. Clearly much

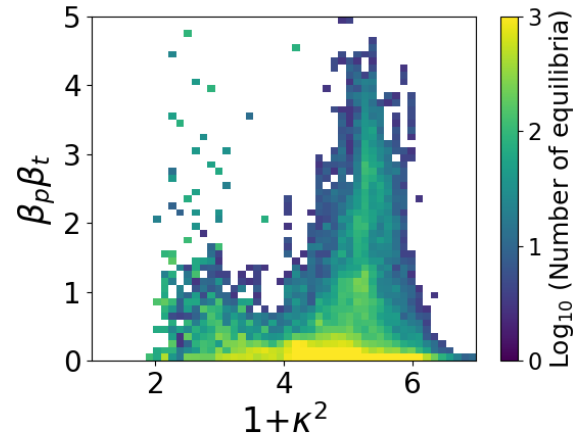


**Figure 7:**  $\beta_p\beta_t$  vs.  $1+\kappa^2$  diagram of the operational space of the first campaign of MAST-U.

of the operation of MAST-U thus far was at low values of the  $\beta_p\beta_t$  product, but the potential for increase is clear. Additionally, a small increase in  $\kappa$  to about 2.45 would give a  $1+\kappa^2$  of 7, the right side of the plot.

### 3.6 Other stability limits

In the present paper we have thus far been discussing global stability limits. Examples of other stability aspects not indicated by the plots shown here are: rotating or tearing MHD modes, and pedestal stability. This is primarily because analysis of such more localized stability issues requires much more detailed calculations and parameters beyond just global equilibrium quantities. However, work is progressing, separately, on this issues as well. For example, the DECAF code also includes the ability to generate and analyze MHD spectrograms [28,29], and this capability has been tested for MAST-U. As another example, high performance MAST-U plasmas have been seen to reach the peeling pedestal stability limit [3]. Work is also underway to analyze MAST-U pedestal stability, as was done for MAST [30].

## Conclusions

MAST-U has completed its first physics campaign, operating in various plasma scenarios with zero, one, or two neutral beams injected, plasma currents levels from 400-800 kA, and in conventional or Super-X divertor configurations. Magnetics only equilibria were reconstructed for many discharges, and these were used to produce operational space diagrams in various spaces. Generally, these diagrams indicate that MAST-U has margins to increase performance in many parameters without yet encountering stability limits, including density towards the Greenwald limit, beta towards global stability limits, and elongation towards vertical stability limits.

## Acknowledgements

The digital data for this paper can be found in <http://arks.princeton.edu/ark:/88435/dsp01j6731612k/>

This work was supported by the U.S. Department of Energy under contract numbers DE-AC02-09CH11466 and DE-SC0018623. The United States Government retains a non-exclusive, paid-up, irrevocable, world-wide license to publish or reproduce the published form of this manuscript, or allow others to do so, for United States Government purposes.

This work has been carried out within the framework of the EUROfusion Consortium, funded by the European Union via

the Euratom Research and Training Programme (Grant Agreement No 101052200 — EUROfusion). Views and opinions expressed are however those of the author(s) only and do not necessarily reflect those of the European Union or the European Commission. Neither the European Union nor the European Commission can be held responsible for them. This work has also been funded by the EPSRC [grant number EP/T012250/1] and the EPSRC Energy Programme [grant number EP/W006839/1].

## References

- [1] Harrison J R *et al* 2019 *Nucl. Fusion* **59** 112011
- [2] Milnes J *et al* 2015 *Fusion Eng. Des.* **96** 42
- [3] Scannell R *et al* 2022 48<sup>th</sup> European Physical Society Conference on Plasma Physics  
<https://indico.fusenet.eu/event/28/contributions/223/>
- [4] Berkery J W *et al* 2021 *Plasma Phys. Control. Fusion* **63** 055014
- [5] Berkery J W *et al* 2017 *Phys. Plasmas* **24** 056103
- [6] Sabbagh S A *et al*, Proceedings of the IAEA Fusion Energy Conference 2018 pp EX/P6-26.
- [7] Appel L C *et al* 2018 *Comput. Phys. Commun.* **223** 1-17
- [8] Kogan L *et al* 2022 48<sup>th</sup> European Physical Society Conference on Plasma Physics  
<https://indico.fusenet.eu/event/28/contributions/165/>
- [9] McArdle G *et al* 2020 *Fusion Eng. Des.* **159** 111764
- [10] Verhaegh K *et al* 2022 *Nucl. Fusion*
- [11] Thornton A, PhD. Thesis, University of York (2011)
- [12] Snape J, PhD. Thesis, University of York (2012)
- [13] Akers R J *et al* 2002 *Phys. Plasmas* **9** 3919
- [14] Buttery R J *et al* 2004 *Nucl. Fusion* **44** 1027
- [15] Hole M J *et al* 2005 *Plasma Phys. Control. Fusion* **47** 581
- [16] Hugill J 1983 *Nucl. Fusion* **23** 331
- [17] Greenwald M *et al* 1988 *Nucl. Fusion* **28** 2199
- [18] Igochine V *Active Control of Magnetohydrodynamic Instabilities in Hot Plasmas*. (Springer, Berlin, 2015)
- [19] Giacomini M *et al* 2022 *Phys. Rev. Lett.* **128** 185003
- [20] Berkery J W *et al* 2014 *Phys. Plasmas* **21** 056112
- [21] Berkery J W *et al* 2020 *Plasma Phys. Control. Fusion* **62** 085007
- [22] Liu Y Q *et al* 2021 *Nucl. Fusion* **61** 116022
- [23] Boyer M D *et al*, 59th Annual Meeting of the APS Division of Plasma Physics 2017 PP11.00041  
<http://meetings.aps.org/link/BAPS.2017.DPP.PP11.41>
- [24] Gates D A *et al* 2006 *Phys. Plasmas* **13** 056122
- [25] Menard J E *et al* 2016 *Nucl. Fusion* **56** 106023
- [26] Boyer M D *et al* 2020 *Nucl. Fusion* **60** 096007
- [27] Miller R L *et al* 1997 *Phys. Plasmas* **4** 1062
- [28] Kaye S M *et al* 2019 *Nucl. Fusion* **59** 112007
- [29] Strait E J *et al* 2019 *Nucl. Fusion* **59** 112012
- [30] Smith S F *et al* 2022 *Plasma Phys. Control. Fusion* **64** 045024